



DTIC FILE COPY

AD-A220 602

Magnetically Insulation Ion Diode with a Gas-Breakdown Plasma Anode

J.B. Greenly, M. Ueda
G.D. Rondeau, and D.A. Hammer

Laboratory of Plasma Studies
Cornell University
Ithaca, New York 14850

LPS 369

June 1987

Research Supported by Office of Naval Research Contract No. N0014-82-K-2059

DISTRIBUTION STATEMENT A
Approved for public release
Distribution is unlimited

DTIC
ELECTE
APR 16 1990
S E D
Co

i

90 04 12

Magnetically Insulated Ion Diode with
a Gas-Breakdown Plasma Anode*

M. Ueda, J.B. Greenly, G.D. Rondeau and D.A. Hammer

Laboratory of Plasma Studies

Cornell University

Ithaca, N.Y. 14853

Abstract

An active anode plasma source has been developed for use in a magnetically insulated ion diode operated on a 10^{10} W pulsed power generator. This source uses an inductive voltage from a single turn coil to break down an annular gas puff produced by a supersonic nozzle. The resulting plasma is magnetically driven toward the radial insulating magnetic field in the diode accelerating gap and stagnates at a well-defined surface after about 300 ns to form a plasma anode layer defined by magnetic flux surfaces. An ion beam is then extracted from this plasma layer by applying a 150 kV, 1 μ s pulse to the accelerating gap. Optimization of the timing of the gas puff, the plasma production discharge and the high voltage pulse has resulted in 1 μ s duration 75-150 keV ion beam pulses with >100 A/cm² peak ion current density over an area of about 400 cm². Up to 5 J/cm² has been collected by a 4 cm² calorimeter. The diode impedance history can be varied so that rising, flat, and falling voltage pulse waveforms can be produced. Streak photographs of beamlets impinging on a scintillator and time integrated targets both show beam divergence angles $\leq 3^\circ$, but under certain operating conditions, large excursions ($\sim 25^\circ$) in mean aiming angle on time scales of 20-200 ns are observed.

Accession For	
NTIS	GRA&I <input checked="" type="checkbox"/>
DTIC	TAB <input type="checkbox"/>
Unannounced <input type="checkbox"/>	
Justification <i>mt</i> <input checked="" type="checkbox"/>	
By _____	
Distribution/	
Availability Code	
Dist	Avail and/or Special
<i>A-1</i>	

Intense pulsed ion beams have potential applications ranging from research directed toward achieving Inertial Confinement Fusion¹ (ICF) at the 10^{14} W level to materials science research² at a power level of about 10^{10} W. An efficient ion diode requires both a method for reducing the electron current in the diode and a source of the desired ion species in a plasma at the anode when the high voltage pulse is applied³. Magnetic insulation³⁻⁵, in which an applied magnetic field perpendicular to the accelerating electric field in an ion diode is used to inhibit the flow of electrons from the cathode to the anode while deflecting the extracted ion beam only slightly, has proven to be an effective technique for electron current reduction in several geometric configurations. In most experiments performed so far, the ion source at the anode in magnetically insulated diodes has been a flashover plasma induced on a dielectric surface by the high voltage pulse that accelerates the ion beam³. Electrons which "leak" across the insulating magnetic field and impinge upon the dielectric surface are also believed to play a major role in the anode plasma formation process⁶. Such "surface flashover anodes" have several shortcomings, including a delay in the generation of the anode plasma relative to the arrival of the voltage pulse, the generation of plasmas with a mixture of ion species from the surface, resulting in beams with several ion species⁷, the generation of neutrals at the anode as well as plasma during the surface breakdown⁸⁻¹⁰, and a limited life which varies from one pulse at the highest power levels¹ to perhaps a few hundred at the 10^9 W/cm² level^{2,10} due to the damage they sustain in each pulse.

In this letter, we present the operating characteristics of an ion diode in which the anode plasma ion source is generated by inductively breaking down an annular gas puff, and magnetically driving the resulting plasma up to a magnetically insulated accelerating gap driven by a 10^{10} W, 1μ s pulsed power generator, LONGSHOT¹¹. This diode has shown itself capable of producing 1μ s duration, 75-150 keV high purity proton beams with >100 A/cm² peak ion current density

over an area of about 400 cm^2 . This represents roughly double the total ion output (both number of ions and energy) achieved on LONGSHOT with a surface flashover anode. By appropriately timing the anode plasma generation relative to the arrival of the LONGSHOT power pulse, ion beam extraction beginning coincident with the start of the voltage pulse has been obtained. Furthermore, no major diode components have required replacement in over 700 pulses with this diode. In general, the gas-breakdown anode plasma ion source has shown itself to be superior to a surface flashover source on LONGSHOT in all categories with the exception of mean beam divergence angle, which is about the same as that produced by using a flashover anode, $\leq 3^\circ$. However, when the plasma prefills the accelerating gap so that beams in excess of 70 A/cm^2 are extracted early in the pulse, we have observed the onset of a macroscopic deterioration of the ion beam quality.

There have been several earlier attempts to provide an anode plasma ion source which overcomes the disadvantages of surface flashover plasmas, such as the plasma filled diode of Mendel¹², and the plasma source used by Humphries et al.¹³ which is a direct ancestor of the source we describe here. Other preionized plasma ion sources in early stages of development for intense ion beam generation were recently described by Isakov et al.¹⁴, Bistritsky et al.¹⁵, and Dreike et al.¹⁶. The actively driven surface flashover anodes (using an energy source independent of the main ion accelerating power pulse) of McClure¹⁷ and Greenly¹¹ addressed the turn-on delay problem, but not the other disadvantages of surface flashover plasma sources.

Figure 1 shows the principal components of the gas-breakdown anode plasma source as used in the LONGSHOT diode. The sequence of events for the system is as follows: The "slow" field coils are energized first, producing the quasi-static magnetic field configuration shown in Fig. 2. Next the puff valve on the diode axis is suddenly opened, and an annular gas puff is delivered to the volume in front of the fast coil (at 15 cm radius) by a supersonic nozzle. The axial puff profile is

sufficiently sharp that the gas pressure in front of the middle of the fast coil can be up to 100 mTorr while the pressure in the ion diode accelerating gap 4 cm away (to the right in Fig. 1) is below 0.5 mTorr. At the optimum moment relative to the time of opening of the puff valve (a function of gas species), the preionizer is energized, followed less than a microsecond later by the fast coil. The latter induces a loop voltage of 17 kV (typical) which rapidly breaks down and drives a current in the preionized gas cloud. (As indicated in Fig. 2, the space just in front of the fast coil is a relatively weak field region before the fast coil is pulsed.) The $\mathbf{J} \times \mathbf{B}$ force, where \mathbf{J} is the current density in the plasma and \mathbf{B} is the magnetic field, on the plasma due to the 1 μ s rise time fast coil magnetic field then drives the plasma toward the ion diode accelerating gap. The plasma stagnates against the magnetic field produced by the slow coils; this field serves to magnetically insulate the accelerating gap of the LONGSHOT ion diode. The precise position of stagnation is determined by the relative strengths of the fast and slow magnetic fields, and is chosen to be near the axial position of the metal anode (item 3 in Fig. 1). It takes about 300 ns for the plasma to be driven to the stagnation point under typical plasma source conditions. The high voltage pulse is then delivered to the accelerating gap. The fundamental difference between this source and that of Humphries¹³ is the presence of the slow field, which confines the plasma both axially and radially during breakdown, allowing order-of-magnitude higher plasma flux to be produced from a similar gas fill.

By varying the time between pulsing the preionizer and the fast coil in the range of about 0.2-1.0 μ s, it is possible to vary the plasma flux delivered to the accelerating gap from about $10^{20}/\text{cm}^2 - \text{s}$ ($20\text{A}/\text{cm}^2$) to about $1.5 \times 10^{21}/\text{cm}^2 - \text{s}$ ($250\text{A}/\text{cm}^2$). These flux measurements were obtained with biased Faraday cups, using a gas puff pressure of 70mTorr (measured with a fast ionization gauge), and 17kV loop voltage. When the system was fired without gas in the puff valve negligible plasma flux was

produced, showing that the gas puff, rather than plasma from surfaces or from the preionizer sparks, produces the output plasma. Varying the gas puff pressure in the range 30-70 mTorr, or the loop voltage over the range 14-23kV changed the plasma flux roughly linearly. Double Langmuir probe measurements as a function of axial position across the stagnation point showed a factor of ten decrease in plasma density over a distance of 3mm, from a peak of about $10^{14}/\text{cm}^3$.

Ion beam production by the LONGSHOT diode employing the gas-breakdown plasma anode was monitored with arrays of single small-aperture biased (-200V) Faraday cups, with a multiple-small-aperture 12 cm^2 biased Faraday cup, with a 4 cm^2 calorimeter, with damage targets (both with and without shadowplates), and with a shadowplate-Pilot-B-scintillator-streak camera combination to obtain time resolved beam optics information.

We first consider basic diode performance (impedance and output current density) obtained with the gas-breakdown anode plasma source. A variety of diode operating conditions can be achieved by adjustment of the amount of plasma delivered to the diode accelerating gap, the time of arrival of the plasma relative to the application of the high voltage pulse from the LONGSHOT generator, and the magnitude of the insulating magnetic field. Figures 3 and 4 show two sample sets of data consisting of the inductively corrected diode voltage, total diode current, and ion current density measured by biased Faraday cups. These data sets illustrate that a flat or rising voltage waveform can be produced by this ion beam source, in contrast to the typical falling voltage waveform obtained using a surface flashover anode plasma ion source. They also illustrate that ion current extraction can be made to begin coincident with the arrival of the high voltage pulse (Fig. 3), or delayed relative to it (Fig. 4). Ion beam pulses of $0.6 - 1 \mu\text{s}$ are routinely obtained. In fact, the voltage pulses shown in Figs. 3 and 4 are as long as for an "open-circuit" shot (i.e.- without injected plasma). Constant diode impedance could be

maintained for 600ns or more with high ion output, as shown by the data of Fig. 3b. Additional data illustrating these points has been presented elsewhere¹⁸.

By averaging the several Faraday cup traces for a shot such as in Figure 4, integrating the average over time and multiplying by 300 cm² (out of the total 400 cm² to correct for radial profile), we estimate that $(1.5 \pm 0.5) \times 10^{17}$ ions with energies greater than 60 keV were produced. A 4 cm² calorimeter measured as much as 5J/cm² in the most energetic shots; this is consistent with 100 A/cm² for 0.5 μ s, or 1×10^{17} 100 keV ions over 300-400 cm². Since Faraday cups are likely to over-estimate the current density while the calorimeter-determined energy density is a lower limit because of surface blowoff from the high ion fluence, these numbers are consistent. It is then possible to estimate the ion current efficiency (ion current/total diode current). Without correcting for possible Faraday cup error, ion current efficiencies up to 70% for 0.5 μ s or more have been obtained. A lower limit of 30% average efficiency over the whole pulse is given by the calorimeter.

Global beam uniformity better than $\pm 35\%$ in both radial and azimuthal directions measured with Faraday cups, has been achieved. Most of this variation is caused by local depressions in gas-puff density where the nozzle is obstructed by bolts holding the inner slow coil (item 6 in Fig. 1). Locally, Faraday cups 1 cm apart agreed to $\pm 10\%$. Gas-puff and preionizer azimuthal uniformity were critical to the attainment of this performance, although the beam uniformity is typically somewhat better than that of the gas puff.

The purity of proton beams produced when hydrogen gas was used in the puff valve was determined by using a pair of biased Faraday cups side by side, one with a 0.5 μ plastic foil and one without. Their signals agreed within the $\pm 10\%$ difference noted for side by side Faraday cups in the last paragraph. Since the low generator voltages, ≤ 200 kV used here, preclude the possibility of any ion other than hydrogen entering the foiled Faraday cup, the beam must be purely composed

of protons, within the $\pm 10\%$ capability of this measurement technique.

Turning now to beam quality, if the high voltage pulse was applied a short time after the plasma was initiated so that little plasma had already reached the accelerating gap, the extracted ion current density, j_i , was $< 70A/cm^2$ for the first 300 ns of the pulse. Streak photographs of beamlets passing through an aperture plate and impinging upon a Pilot-B scintillator showed beam divergence of $< 3^\circ$ in agreement with time integrated shadowbox targets. No time dependent beam aiming variation was observed. A streak photograph of such a shot is shown in Figure 5a. However, when the voltage pulse began a long time after initiation of the plasma source so that the gap had a substantial plasma prefill, the ion beam was less uniform. In local areas of the diode giving high ion current density ($> 70A/cm^2$) early in the pulse ($< 300ns$), substantial time-dependent beamlet variation was observed. The streaks showed beamlet motion and spreading of $20-30^\circ$ on a time scale of tens to hundreds of nanoseconds, as shown in Figure 5b. Even in these cases, the beam optics sometimes improved late in the pulse, as can be seen in Fig. 5b. The beam degradation was not observed in experiments with a metal screen attached to the anode contact and extending radially inward over the entire diode area.

The wide range of operating regimes available with this diode is clearly determined by the anode plasma characteristics. Prompt, or delayed, turn-on is observed when plasma is supplied early, or late, relative to the accelerating voltage pulse. Diode impedance is determined by the density and distribution of plasma in the gap at the beginning of the pulse, and thereafter by the plasma flux which continues to be driven into the gap. The balance between extracted ion beam current density and injected plasma flux determines whether the gap impedance rises, falls or remains constant. The gross ion beam aiming and divergence variations observed are a local phenomenon, most likely the result of a locally uneven anode plasma sup-

ply, producing a nonuniform plasma prefill in the gap. Current-driven instability of the anode plasma seems unlikely to be the cause, since equally high ion current density could be extracted later in the pulse without degradation of optics. The good beam optics observed with the metal screen anode insert could indicate that the conducting screen suppresses interchange instability of the plasma as it is being driven into the diode insulating magnetic flux.

All of these observations suggest that the position, shape, and time-variation of an effective anode "surface" defined by the front of the plasma is a useful concept in understanding the gap dynamics. The behavior of this surface, interacting with the electron dynamics of the virtual cathode, and modified by a final diode closure possibly occurring outside the gap itself, together determine the overall diode impedance history. Two indirect measures of the anode surface position were made. First, the azimuthal deflection angle of the extracted ion beam is a measure of the total magnetic flux crossed by the beam ions, and thus can determine the flux surface on which the anode surface sits. This angle was measured as a function of time, and showed that the anode surface position indeed varied depending on the balance of plasma supply and beam extraction. Second, a time-dependent effective anode-cathode gap could be calculated from the diode voltage and ion beam current density, assuming a Child-Langmuir gap. This gap is a function of both anode and virtual cathode positions. Its variation was seen to depend strongly on anode plasma parameters, and is certainly not solely a function of virtual cathode dynamics in this diode.

A fundamental difference between this behavior and that of the same diode with a standard surface-flashover anode is that large enhancement (factor of >30) of the ion current density over Child-Langmuir current for the bare gap (3 A/cm^2) is seen only near the end of the pulse just before gap shorting with the solid anode. These large enhancements can occur early, and persist for nearly a microsecond with

the plasma anode. This difference also suggests strongly that anode surface motion, as well as motion of the virtual cathode, is responsible for the small effective gap at these high current enhancements.

Data and theoretical considerations supporting these and other inferences about plasma physics and gap dynamics in this diode will be discussed in detail in a future publication.

Finally we note two additional observations. First, because the puff valve can in principle be filled with any gas, it should be possible to produce pure beams of many different ion species. In fact, we have produced 100 A/cm^2 beams using a nitrogen gas puff. Second, no major diode components required replacement in over 700 shots with the gas-breakdown anode plasma source, confirming the possibility that this ion beam source is capable of repetitive pulse, long lived operation.

We wish to thank Edl Schamiloglu for his assistance with the double Langmuir probe density measurements. This research was supported by ONR contract # N00014-82-2059.

References

1. J.P. VanDevender and D.L. Cook, *Science* **232**, 831 (1986).
2. W.K. Chu, *Nucl. Instr. and Methods* **194**, 443 (1982).
3. See, for example, S. Humphries Jr., *Nucl. Fusion* **20**, 1549 (1980).
4. F. Winterberg, *Phys. Rev.* **174**, 212 (1968).
5. P. Dreike, C. Eichenberger, S. Humphries, Jr., and R.N. Sudan, *J. Appl. Phys.* **47**, 85 (1976)
6. D.J. Johnson, J.P. Quintenz and M.A. Sweeney, *J. Appl. Phys.* **57**, 794 (1985).
7. J.M. Neri, Ph.D. thesis Cornell university, 1983, (unpublished).
8. D.S. Prono, H. Ishizuka, E.P. Lee, B.W. Stallard and W.C. Turner, *J. Appl. Phys.* **52**, 3004 (1981).
9. J.B. Greenly and Y. Nakagawa, Cornell University LPS report #303, June, 1987 (submitted to *J. Appl. Phys.*).
10. R. Pal and D.A. Hammer, *Phys. Rev. Lett.* **50**, (1982).
11. J.B. Greenly, Cornell University Laboratory of Plasma Studies report #315, (1983).
12. C.W. Mendel and G.S. Mills, *J. Appl. Phys.* **53**, 7265 (1983).
13. S. Humphries jr., J.R. Freeman, John B. Greenly, G.W. Kuswa, C.W. Mendel, J.W. Poukey and D.M. Woodall, *J. Appl. Phys.* **51**, 1876 (1982).
14. I.F. Isakov, E.I. Logachev, U.S. Lopatin, S.A. Pechenkin, G.E. Remnev, *Proc Sixth Int. Conf. on High Power Particle Beams*, p. 77, (Kobe, Japan, June 1986).
15. V.M. Bistritskii, A.N. Didenko, and A.V. Petrov, *Proc. Sixth Int. Conf. on High Power Particle Beams*, p. 176, (Kobe, Japan, June 1986).
16. P.L. Dreike, D.M. Mattox, G.C. Tisone and E. Dawson, *Bull. Am. Phys. Soc.* **31**, 1509 (1986).
17. G.W. McClure, L. Baker, J.A. Webb and C.J. Cianciabella, Sandia National Laboratories Report SAND 82-0340, Sept. (1982).
18. J.B. Greenly, M. Ueda, G.D. Rondeau and D.A. Hammer, *Proc Sixth Int. Conf. on High Power Particle Beams*, p.196, (Kobe, Japan, June 1986).

Figure Captions

Figure 1.

The LONGSHOT diode with gas-breakdown plasma anode: Aluminum cathode pieces (1,2) and flux-penetrable anode contacts (3,4) define the diode accelerating gap, magnetically insulated by the slow field coils (5,6,7). Coil (7) is inductively decoupled from the fast coil (8) by a plate (9) with suitable intermediate flux-penetration time. The anode components are mounted on a base plate (10) connected to the LONGSHOT generator output interface (not shown). The fast gas valve plenum (11) is opened magnetically by a pulsed coil (12). The gas puff enters an axial channel (13), then expands radially in the supersonic nozzle formed by a front plate (14) and the epoxy casting (15) containing the fast coil. Preionizers (16) are an array of spark gaps on an epoxy surface.

Figure 2.

Magnetic flux lines produced by the slow (diode insulating field) coils (5,6,7). Components are numbered as in Figure 1.

Figure 3.

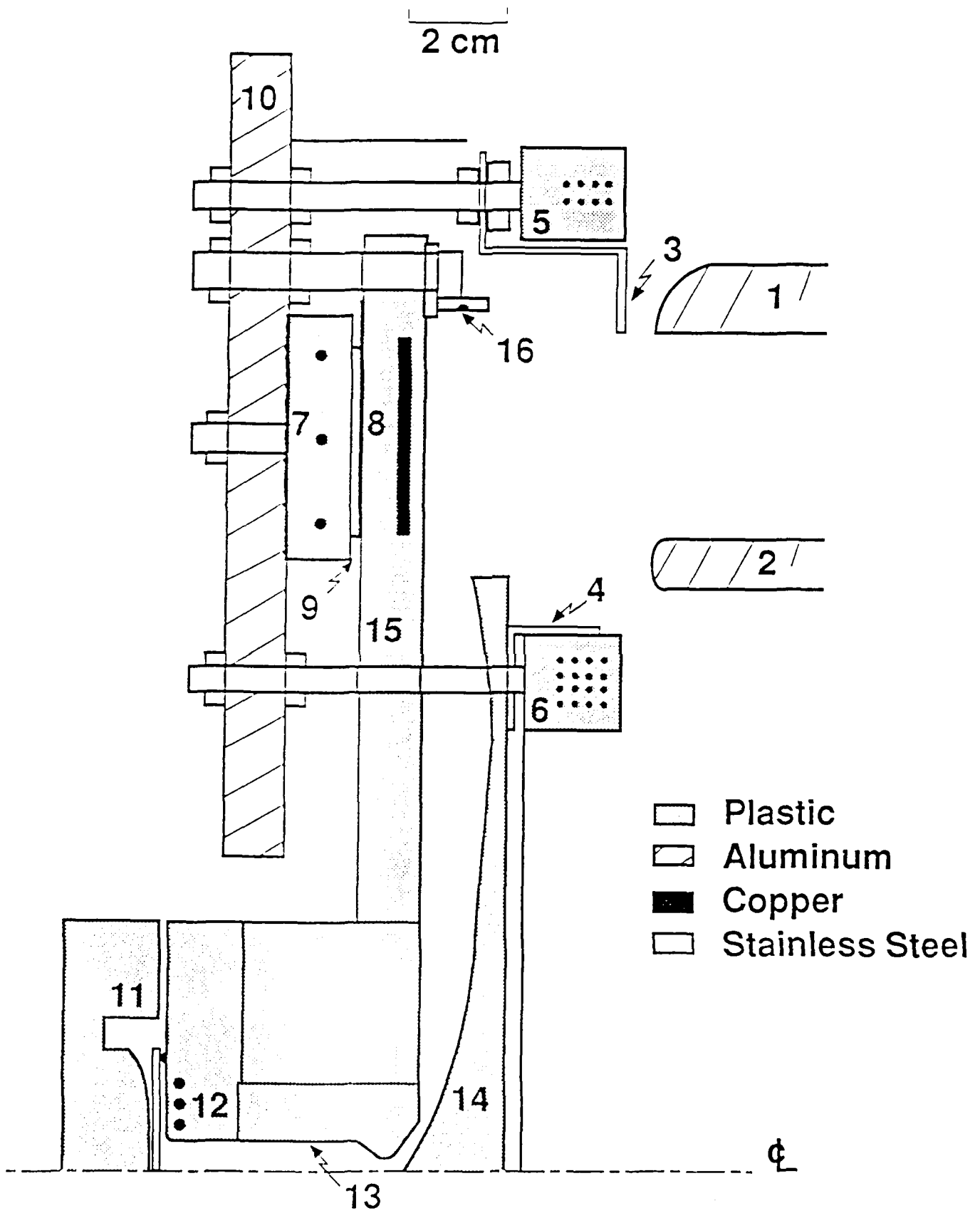
Diode accelerating voltage, total diode current, and ion beam current density measured by four biased Faraday cups spaced around the diode azimuth, for a shot with moderate plasma source flux and a relatively long delay between fast coil and diode voltage pulses.

Figure 4.

Diode accelerating voltage, total diode current, and two Faraday cup signals for a shot with high plasma source flux and short delay between fast coil and diode voltage pulses. Also plotted is the calculated diode impedance versus time measured from time (A) on the voltage trace.

Figure 5.

A schematic diagram showing the geometry of: the streak camera (C); viewing a Pilot-B scintillator sheet (S); struck by ion beamlets selected by the aperture plate (P) which blocks the beam emerging from the (A-K) diode gap. The scintillator has a thin front aluminum coating to exclude diode light, and must be replaced each shot. Streak photographs are shown with corresponding traces of diode voltage and of ion current density measured by a Faraday cup placed near the aperture plate. Streak start is indicated by arrows on the photograph and traces. These data are shown for a shot (a) with good beam optics, and for a shot (b) with severely degraded optics.



2 cm

10

5

3

1

16

7

8

9

15

4

6

11

12

14

13

ϕ

